

First Observation of $\Upsilon(1D)$ States*

S. E. Csorna,¹ I. Danko,¹ G. Bonvicini,² D. Cinabro,² M. Dubrovin,² S. McGee,²
A. Bornheim,³ E. Lipeles,³ S. P. Pappas,³ A. Shapiro,³ W. M. Sun,³ A. J. Weinstein,³
R. Mahapatra,⁴ R. A. Briere,⁵ G. P. Chen,⁵ T. Ferguson,⁵ G. Tatishvili,⁵ H. Vogel,⁵
N. E. Adam,⁶ J. P. Alexander,⁶ K. Berkelman,⁶ V. Boisvert,⁶ D. G. Cassel,⁶
P. S. Drell,⁶ J. E. Duboscq,⁶ K. M. Ecklund,⁶ R. Ehrlich,⁶ R. S. Galik,⁶ L. Gibbons,⁶
B. Gittelmann,⁶ S. W. Gray,⁶ D. L. Hartill,⁶ B. K. Heltsley,⁶ L. Hsu,⁶ C. D. Jones,⁶
J. Kandaswamy,⁶ D. L. Kreinick,⁶ A. Magerkurth,⁶ H. Mahlke-Krüger,⁶ T. O. Meyer,⁶
N. B. Mistry,⁶ E. Nordberg,⁶ J. R. Patterson,⁶ D. Peterson,⁶ J. Pivarski,⁶ D. Riley,⁶
A. J. Sadoff,⁶ H. Schwarthoff,⁶ M. R. Shepherd,⁶ J. G. Thayer,⁶ D. Urner,⁶
G. Viehhauser,⁶ A. Warburton,⁶ M. Weinberger,⁶ S. B. Athar,⁷ P. Avery,⁷
L. Brea-Newell,⁷ V. Potlia,⁷ H. Stoeck,⁷ J. Yelton,⁷ G. Brandenburg,⁸ D. Y.-J. Kim,⁸
R. Wilson,⁸ K. Benslama,⁹ B. I. Eisenstein,⁹ J. Ernst,⁹ G. D. Gollin,⁹ R. M. Hans,⁹
I. Karliner,⁹ N. Lowrey,⁹ C. Plager,⁹ C. Sedlack,⁹ M. Selen,⁹ J. J. Thaler,⁹
J. Williams,⁹ K. W. Edwards,¹⁰ R. Ammar,¹¹ D. Besson,¹¹ X. Zhao,¹¹ S. Anderson,¹²
V. V. Frolov,¹² Y. Kubota,¹² S. J. Lee,¹² S. Z. Li,¹² R. Poling,¹² A. Smith,¹²
C. J. Stepaniak,¹² J. Urheim,¹² Z. Metreveli,¹³ K.K. Seth,¹³ A. Tomaradze,¹³
P. Zweber,¹³ S. Ahmed,¹⁴ M. S. Alam,¹⁴ L. Jian,¹⁴ M. Saleem,¹⁴ F. Wappler,¹⁴
E. Eckhart,¹⁵ K. K. Gan,¹⁵ C. Gwon,¹⁵ T. Hart,¹⁵ K. Honscheid,¹⁵ D. Hufnagel,¹⁵
H. Kagan,¹⁵ R. Kass,¹⁵ T. K. Pedlar,¹⁵ J. B. Thayer,¹⁵ E. von Toerne,¹⁵ T. Wilksen,¹⁵
M. M. Zoeller,¹⁵ H. Muramatsu,¹⁶ S. J. Richichi,¹⁶ H. Severini,¹⁶ P. Skubic,¹⁶
S.A. Dytman,¹⁷ J.A. Mueller,¹⁷ S. Nam,¹⁷ V. Savinov,¹⁷ S. Chen,¹⁸ J. W. Hinson,¹⁸
J. Lee,¹⁸ D. H. Miller,¹⁸ V. Pavlunin,¹⁸ E. I. Shibata,¹⁸ I. P. J. Shipsey,¹⁸
D. Cronin-Hennessy,¹⁹ A.L. Lyon,¹⁹ C. S. Park,¹⁹ W. Park,¹⁹ E. H. Thorndike,¹⁹
T. E. Coan,²⁰ Y. S. Gao,²⁰ F. Liu,²⁰ Y. Maravin,²⁰ R. Stroynowski,²⁰ M. Artuso,²¹
C. Boulahouache,²¹ K. Bukin,²¹ E. Dambasuren,²¹ K. Khroustalev,²¹ R. Mountain,²¹
R. Nandakumar,²¹ T. Skwarnicki,²¹ S. Stone,²¹ J.C. Wang,²¹ and A. H. Mahmood²²

(CLEO Collaboration)

¹*Vanderbilt University, Nashville, Tennessee 37235*

²*Wayne State University, Detroit, Michigan 48202*

³*California Institute of Technology, Pasadena, California 91125*

⁴*University of California, Santa Barbara, California 93106*

⁵*Carnegie Mellon University, Pittsburgh, Pennsylvania 15213*

⁶*Cornell University, Ithaca, New York 14853*

⁷*University of Florida, Gainesville, Florida 32611*

⁸*Harvard University, Cambridge, Massachusetts 02138*

⁹*University of Illinois, Urbana-Champaign, Illinois 61801*

¹⁰*Carleton University, Ottawa, Ontario, Canada K1S 5B6
and the Institute of Particle Physics, Canada M5S 1A7*

¹¹*University of Kansas, Lawrence, Kansas 66045*

¹²*University of Minnesota, Minneapolis, Minnesota 55455*

¹³*Northwestern University, Evanston, Illinois 60208*

¹⁴*State University of New York at Albany, Albany, New York 12222*

¹⁵*Ohio State University, Columbus, Ohio 43210*

¹⁶*University of Oklahoma, Norman, Oklahoma 73019*

¹⁷*University of Pittsburgh, Pittsburgh, Pennsylvania 15260*

¹⁸*Purdue University, West Lafayette, Indiana 47907*

¹⁹*University of Rochester, Rochester, New York 14627*

²⁰*Southern Methodist University, Dallas, Texas 75275*

²¹*Syracuse University, Syracuse, New York 13244*

²²*University of Texas - Pan American, Edinburg, Texas 78539*

(Dated: July 19, 2002)

Abstract

The CLEO III experiment has recently accumulated a large statistics sample of $4.73 \cdot 10^6$ $\Upsilon(3S)$ decays. We present the first evidence for the production of the triplet $\Upsilon(1D)$ states in the four-photon cascade, $\Upsilon(3S) \rightarrow \gamma\chi_b(2P)$, $\chi_b(2P) \rightarrow \gamma\Upsilon(1D)$, $\Upsilon(1D) \rightarrow \gamma\chi_b(1P)$, $\chi_b(1P) \rightarrow \gamma\Upsilon(1S)$, followed by the $\Upsilon(1S)$ annihilation to e^+e^- or $\mu^+\mu^-$. The signal has a significance of 9.7 standard deviations. The measured product branching ratio for these five decays, $(3.3 \pm 0.6 \pm 0.5) \cdot 10^{-5}$, is consistent with the theoretical estimates. We see a 6.8 standard deviation signal for a state with a mass of 10162.2 ± 1.6 MeV/ c^2 , consistent with the $\Upsilon(1D_2)$ assignment.

We also present improved measurements of the $\Upsilon(3S) \rightarrow \pi^0\pi^0\Upsilon(1S)$ branching ratio and the associated di-pion mass distribution.

*Submitted to the 31st International Conference on High Energy Physics, July 2002, Amsterdam

I. INTRODUCTION

Long-lived $b\bar{b}$ states are especially well suited for testing QCD via lattice calculations [1] and effective theories of strong interactions, like potential models [2]. The narrow triplet S states, $\Upsilon(1S)$, $\Upsilon(2S)$ and $\Upsilon(3S)$, were discovered in 1977 in proton-nucleus collisions at Fermilab [3]. Later, they were better resolved and studied at various e^+e^- storage rings. Six triplet P states, $\chi_b(2P_J)$ and $\chi_b(1P_J)$ with $J = 0, 1, 2$, were discovered in radiative decays of the $\Upsilon(3S)$ and $\Upsilon(2S)$ in 1982 [4] and 1983 [5], respectively. There has been no observations of new narrow $b\bar{b}$ states since then despite the large number of such states predicted below the open flavor threshold (see Fig. 1).

In this paper, we present the first observation of the $\Upsilon(1D)$ states. Except for the yet unobserved $\Upsilon(2D)$ states, these are the only long-lived $L = 2$ mesons in nature. They are produced in a two-photon cascade starting from the $\Upsilon(3S)$ resonance: $\Upsilon(3S) \rightarrow \gamma\chi_b(2P_J)$, $\chi_b(2P_J) \rightarrow \gamma\Upsilon(1D)$. To suppress photon backgrounds from π^0 s, which are copiously produced in gluonic annihilation of the $b\bar{b}$ states, we select events with two more subsequent photon transitions, $\Upsilon(1D) \rightarrow \gamma\chi_b(1P_J)$, $\chi_b(1P_J) \rightarrow \gamma\Upsilon(1S)$, followed by the $\Upsilon(1S)$ annihilation to either e^+e^- or $\mu^+\mu^-$ (see Fig. 1). The product branching ratio for these five decays in sequence was predicted by Godfrey and Rosner [7] to be $3.76 \cdot 10^{-5}$.

The CLEO III experiment has recently accumulated $4.73 \cdot 10^6$ $\Upsilon(3S)$ decays, which makes the detection of such rare processes possible. The CLEO III sample constitutes roughly a ten-fold increase in $\Upsilon(3S)$ statistics compared to the CLEO II data set [8], and roughly a four-fold increase compared to the integrated CUSB data set [9]. Thanks to the good granularity and the large solid angle of the CLEO CsI(Tl) calorimeter, the CLEO III detection efficiency for these final states is about 4.5 times larger than in the CUSB detector. Even though the CLEO III calorimeter is essentially the same as in the CLEO II detector [10], the photon selection efficiency and detector resolution were improved in the endcaps and in part of the barrel calorimeter by the installation of a new, lower-mass, tracking system [11]. Another change was the replacement of the time-of-flight system by a RICH detector in the barrel part. Finally, the calorimeter endcaps were restacked and moved farther away from the interaction point to accommodate a new, higher luminosity, interaction point optics.

II. DATA SELECTION

We select events with exactly four photons and two oppositely charged leptons. The leptons must have momenta of at least $3.75 \text{ GeV}/c$. We distinguish between electrons and muons by their energy deposition in the calorimeter. Electrons must have a high ratio of energy observed in the calorimeter to the momentum measured in the tracking system ($E/p > 0.7$). Muons are identified as minimum ionizing particles, and required to leave $150 - 550 \text{ MeV}$ of energy in the calorimeter. Stricter muon identification does not reduce background in the final sample, since all significant background sources contain muons. Each photon must have at least 60 MeV of energy. We also ignore all photons below 180 MeV in the calorimeter region closest to the beam, because of the spurious photons generated by beam-related backgrounds. The total momentum of all photons and leptons in each event must be balanced to within $300 \text{ MeV}/c$. The invariant mass of the two leptons must be consistent with the $\Upsilon(1S)$ mass within $\pm 300 \text{ MeV}/c^2$. Much better identification of the $\Upsilon(1S)$ resonance is obtained by measuring the mass of the system recoiling against the four photons. The average resolution of the recoil mass is $17 \text{ MeV}/c^2$. Cuts on the recoil

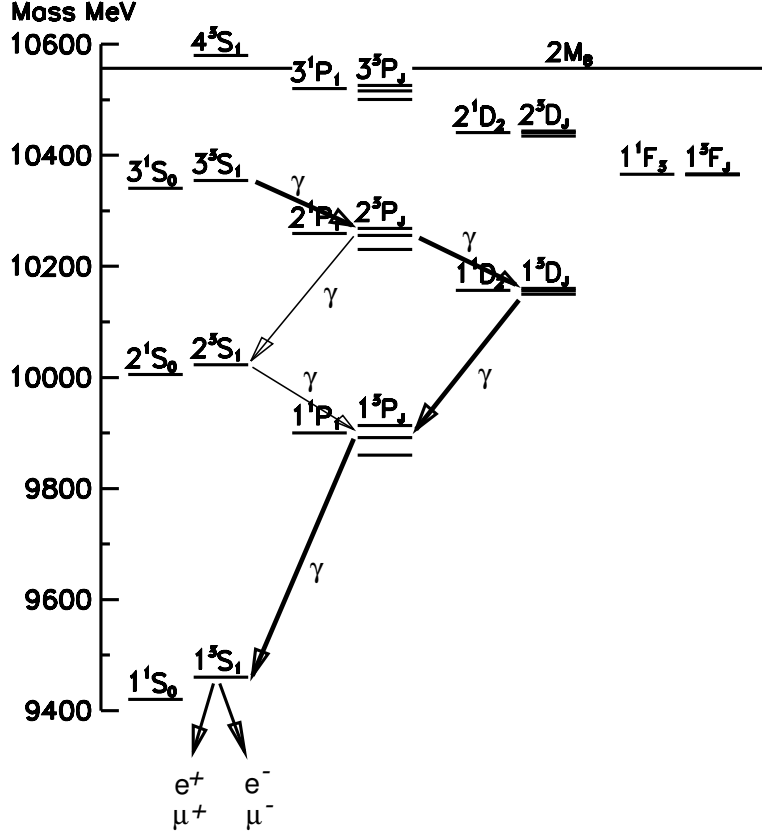


FIG. 1: $b\bar{b}$ mass levels as predicted by one of the potential models. The levels are denoted by their spectroscopic labels, $n^{2S+1}L_J$, where n is the radial quantum number ($n = 1, 2, \dots$), S is the total quark spin ($S = 0$ spin singlets, $S = 1$ spin triplets), L is the orbital angular momentum ($L = S, P, D, \dots$) and J is the total angular momentum of the state ($\vec{J} = \vec{S} + \vec{L}$). The four-photon transition sequence via the $\Upsilon(1D)$ states is shown. An alternative route in four-photon cascade via the $\Upsilon(2S)$ state is also displayed.

mass are described below. The mass resolution of the produced $\Upsilon(1D)$ state depends on the measurement of the energies of the two lowest energy photons in the event. Thus, we require that at least one of them is detected in the barrel part of the calorimeter, where the energy resolution is best. The energy resolution as determined by the fit to the $\Upsilon(3S) \rightarrow \gamma\chi_b(2P_J)$ photon lines is $\sigma_{E_\gamma} = (4.6 \pm 0.2)$ MeV for $E_\gamma = 100$ MeV [12].

III. $\Upsilon(3S) \rightarrow \pi^0\pi^0\Upsilon(1S)$ TRANSITIONS

The most prominent signal among $\Upsilon(3S) \rightarrow \gamma\gamma\gamma\gamma\Upsilon(1S)$ decays are $\Upsilon(3S) \rightarrow \pi^0\pi^0\Upsilon(1S)$ transitions. To identify these decays, we try all three combinations of four photons into two-photon pairs. We find the minimal π^0 mass deviation chi-squared among these combinations: $\chi_{\pi^0\pi^0}^2 = \min \left\{ [(M_{\gamma\gamma}^{ij} - M_{\pi^0})/\sigma_{M_{\gamma\gamma}^{ij}}]^2 + [(M_{\gamma\gamma}^{kl} - M_{\pi^0})/\sigma_{M_{\gamma\gamma}^{kl}}]^2 \right\}$. After the requirement $\chi_{\pi^0\pi^0}^2 < 6$, the deviation of the four-photon recoil mass from the $\Upsilon(1S)$ mass, $\Delta M = M_{recoil\ 4\gamma} - M_{\Upsilon(1S)}$, is found. The distribution of the ratio, $\Delta M/\sigma(\Delta M)$, where $\sigma(\Delta M)$ is the expected recoil mass resolution, is plotted in Fig. 2. As can be seen from the

sidebands of this distribution, backgrounds from non- $\Upsilon(3S) \rightarrow \Upsilon(1S)$ transitions (e.g. radiative Bhabha and μ -pair events) are small. We subtract this background by fitting the recoil mass distribution with the signal shape extracted from the Monte Carlo simulations. The fit is also shown in Fig. 2. We observe 737 ± 28 events with an efficiency of 13.6%. The efficiency was determined from the Monte Carlo simulations. This sample contains a small fraction, 0.9%, of photon cascade background that we estimate from the cross-efficiency determined with the Monte Carlo (below 1%) and the branching ratios measured from the data, as described below. After the background subtraction, we obtain the following result for the product branching ratio: $\mathcal{B}(\Upsilon(3S) \rightarrow \pi^0\pi^0\Upsilon(1S)) \cdot \mathcal{B}(\Upsilon(1S) \rightarrow l^+l^-) = (5.67 \pm 0.22 \pm 0.35) \cdot 10^{-4}$. The first error is statistical and the second is systematic. The systematic error is dominated by uncertainties in the Monte Carlo simulation of the selection efficiency. It was determined by varying the selection criteria. Here, $\mathcal{B}(\Upsilon(1S) \rightarrow l^+l^-)$ means either $\mathcal{B}(\Upsilon(1S) \rightarrow e^+e^-)$ or $\mathcal{B}(\Upsilon(1S) \rightarrow \mu^+\mu^-)$, since these two branching ratios should be equal from lepton universality. Using the world average value [13], $\mathcal{B}(\Upsilon(1S) \rightarrow l^+l^-) = (2.43 \pm 0.06)\%$, we can unfold our result for $\mathcal{B}(\Upsilon(3S) \rightarrow \pi^0\pi^0\Upsilon(1S)) = (2.33 \pm 0.09 \pm 0.16)\%$. This result is consistent with, but more precise, than previous measurements by CLEO II [14], $(2.03 \pm 0.28 \pm 0.19)\%$, and CUSB [9], $(2.3 \pm 0.4 \pm 0.3)\%$. The efficiency-corrected invariant mass distribution of the two-pion system is shown in Fig. 3. As in the previous measurements, some dynamical structure is observed in this distribution.

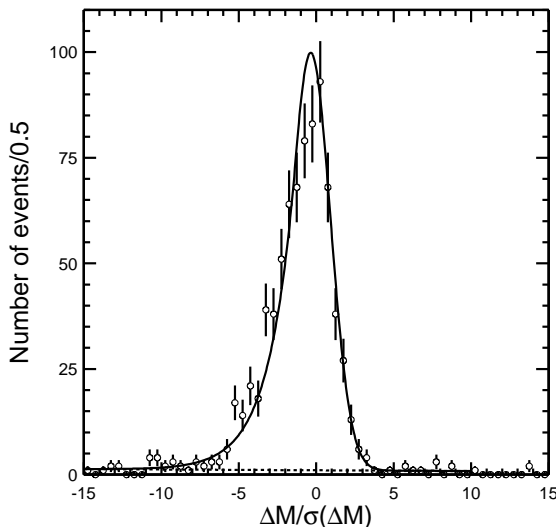


FIG. 2: Distribution of the recoil mass deviation from the $\Upsilon(1S)$ mass for the $\Upsilon(3S) \rightarrow \pi^0\pi^0\Upsilon(1S)$ candidate events. The solid-line represents the fit of a signal peak on top of the linear background (dashed-line).

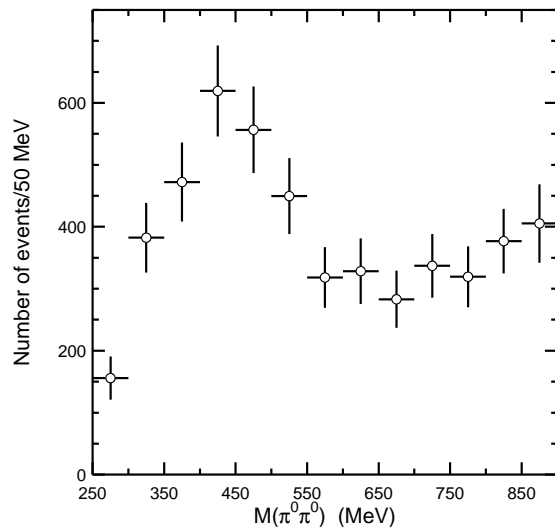


FIG. 3: Efficiency-corrected distribution of the $\pi^0\pi^0$ invariant mass observed in the data.

The determination of $\mathcal{B}(\Upsilon(3S) \rightarrow \pi^0\pi^0\Upsilon(1S))$ presented above serves as a good cross-check of our experimental techniques. In a separate paper submitted to this conference [12], we also present the analysis of the two-photon cascades between the $\Upsilon(3S)$ and the $\Upsilon(1S)$ or $\Upsilon(2S)$. Branching ratios for two-photon cascades via $\chi_b(2P)$ and $\chi_b(1P)$ states

were determined with improved precision compared to previous experiments. These data, together with the $\pi^0\pi^0$ transitions, were used to obtain the calibration of absolute photon energies in the 60 – 800 MeV range. Using the well known masses of the $\Upsilon(1S)$, $\Upsilon(2S)$ and $\Upsilon(3S)$ [13], together with the recoil mass distributions like the one shown in Fig. 2, we calibrated the photon energies to a precision of 0.35%. The photon energies observed in the two-photon cascade data for $\Upsilon(3S) \rightarrow \gamma\chi_b(2P_J)$ agreed well with the previous measurements. Thus, the systematic effects in both rate and photon energy measurements are well under control.

IV. EVIDENCE FOR THE $\Upsilon(1D)$ STATES

To look for four-photon cascades between the $\Upsilon(3S)$ and $\Upsilon(1S)$, we must suppress backgrounds from the $\pi^0\pi^0$ transitions. We first require, $\chi_{\pi^0\pi^0}^2 > 6$. In addition, every photon pair must have an invariant mass at least two standard deviations away from the nominal π^0 mass.

To look for $\Upsilon(1D)$ events, we constrain events to be consistent with a photon cascade from the $\Upsilon(3S)$ to the $\Upsilon(1S)$ via one of the $\chi_b(2P_J)$ and one of the $\chi_b(1P_J)$ states ($J = 0, 1, 2$). The masses of the P states are well known from other measurements [13]. For each J_{2P} , J_{1P} combination we calculate a chi-squared:

$$\chi_{1D, J_{2P}, J_{1P}}^2(M_{\Upsilon(1D)}) = \sum_{j=1}^4 \left(\frac{E_{\gamma j} - E_{\gamma j}^{expected}(M_{\Upsilon(1D)}, J_{2P}, J_{1P})}{\sigma_{E_{\gamma j}}} \right)^2,$$

where $E_{\gamma j}$ are the measured photon energies; $E_{\gamma j}^{expected}$ are the expected photon energies from the masses of the $b\bar{b}$ states and the measured photon directions in the cascade. The masses of the $\Upsilon(1D)$ states are not known. Therefore, we minimize the above chi-squared with respect to $M_{\Upsilon(1D)}$ which is allowed to vary for each event. The above formalism requires that we know how to order the four photons in the cascade. While the highest energy photon must be due to the fourth transition, and the second highest energy photon must be due to the third transition, there is sometimes an ambiguity in the assignment of the two lowest energy photons to the first two transitions, since the range of photon energies in the $\Upsilon(3S) \rightarrow \gamma\chi_b(2P_J)$ decay overlaps the possible photon energy range in the $\chi_b(2P_J) \rightarrow \gamma\Upsilon(1D)$ transition. We choose the combination that minimizes the above chi-squared. There are nine possible combinations of J_{2P} , J_{1P} spins. We try all of them and choose the one that produces the smallest chi-squared, $\chi_{1D}^2 = \min \chi_{1D, J_{2P}, J_{1P}}^2$.

In addition to the four-photon cascade via the $\Upsilon(1D)$ states, our data contain events with the four-photon cascade via the $\Upsilon(2S)$ state: $\Upsilon(3S) \rightarrow \gamma\chi_b(2P_J)$, $\chi_b(2P_J) \rightarrow \gamma\Upsilon(2S)$, $\Upsilon(2S) \rightarrow \gamma\chi_b(1P_J)$, $\chi_b(1P_J) \rightarrow \gamma\Upsilon(1S)$, $\Upsilon(1S) \rightarrow l^+l^-$ (see Fig. 1). This is a coincidence of the two-photon cascades, $\Upsilon(3S) \rightarrow \gamma\gamma\Upsilon(2S)$ and $\Upsilon(2S) \rightarrow \gamma\gamma\Upsilon(1S)$, which were experimentally observed in the two-photon cascades detected in the $\Upsilon(3S)$ [12] and $\Upsilon(2S)$ data [15]. The product branching ratio for this entire decay sequence (including $\Upsilon(1S) \rightarrow l^+l^-$) is predicted by Godfrey and Rosner [7] to be $3.84 \cdot 10^{-5}$, thus comparable to the predicted $\Upsilon(1D)$ production rate. Combining the measured rates for $\mathcal{B}(\Upsilon(3S) \rightarrow \gamma\gamma\Upsilon(2S)) \cdot \mathcal{B}(\Upsilon(2S) \rightarrow l^+l^-)$ [12] and $\mathcal{B}(\Upsilon(2S) \rightarrow \gamma\gamma\Upsilon(1S)) \cdot \mathcal{B}(\Upsilon(1S) \rightarrow l^+l^-)$ [15] with the measurement of $\mathcal{B}(\Upsilon(2S) \rightarrow \mu^+\mu^-)$ [13], we obtain a factor 1.9 ± 0.3 higher value. In these events, the second highest energy photon is due to the second photon transition (see Fig. 1). Unfortunately, these events can be sometimes confused with the $\Upsilon(1D)$

events due to the limited experimental energy resolution. The second and third photon transitions in the $\Upsilon(2S)$ cascade sequence can be mistaken for the third and second transition in the $\Upsilon(1D)$ cascade sequence. Therefore, it is important to suppress the $\Upsilon(2S)$ cascades. We achieve this by finding the J_{2P}, J_{1P} combination that minimizes the associated chi-squared for the $\Upsilon(2S)$ hypothesis, $\chi_{2S}^2 = \min \chi_{2S, J_{2P}, J_{1P}}^2$, where χ_{2S}^2 is exactly analogous to χ_{1D}^2 with the $M_{\Upsilon(1D)}$ replaced with $M_{\Upsilon(2S)}$. We then require $\chi_{2S}^2 > 12$. Notice that the masses of all intermediate states are known for the $\Upsilon(2S)$ cascade, thus this variable is more constraining than χ_{1D}^2 . To further suppress the $\Upsilon(2S)$ cascade events, we construct a quasi-chi-squared variable, χ_{2S}^{2+} , that sums in quadrature only positive deviations of the measured photon energies from their expected values. This variable is less sensitive to fluctuations in the longitudinal and transverse energy leakage in photon showers that sometimes produce large negative energy deviations and correspondingly a large χ_{2S}^2 value. With the additional cut $\chi_{2S}^{2+} > 3$, the cross-efficiency for $\Upsilon(2S)$ events is reduced to 0.7% and is further suppressed by a factor of two when a cut of $\chi_{1D}^2 < 10$ is required.

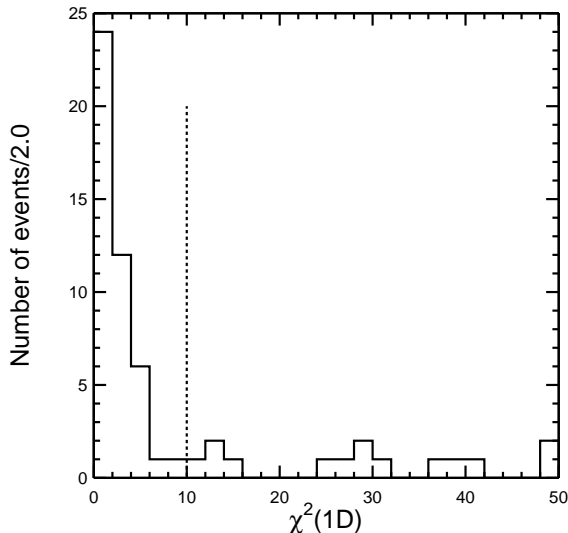


FIG. 4: χ_{1D}^2 distribution for the data. The cut value used for the mass analysis is indicated by the vertical bar.

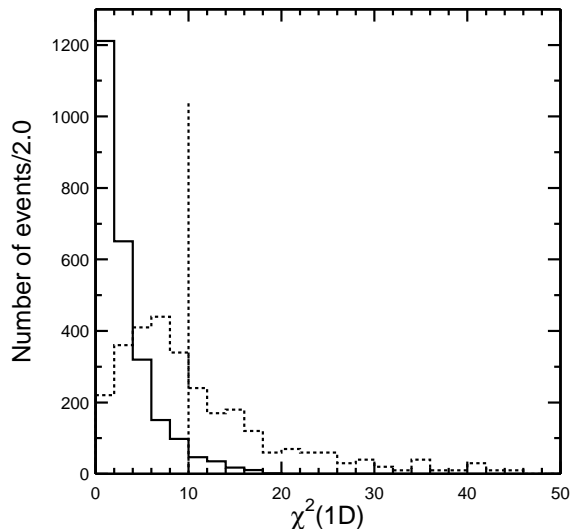


FIG. 5: χ_{1D}^2 distribution for the $\Upsilon(1D)$ (solid-histogram) and $\Upsilon(2S)$ cascade Monte Carlo (dashed-histogram). The latter distribution was scaled up by a factor of 10 to be visible on the scale of the signal Monte Carlo.

The data χ_{1D}^2 distribution, after we require the four-photon recoil mass to be between -4 and $+3$ standard deviations from the nominal $\Upsilon(1S)$ mass, is shown in Fig. 4. A narrow peak near zero is observed, just as expected for $\Upsilon(1D)$ events. The signal Monte Carlo distribution for $\Upsilon(1D)$ events is shown in Fig. 5. The background Monte Carlo distribution for the $\Upsilon(2S)$ cascades, after a factor of 10 enhancement relative to the $\Upsilon(1D)$ normalization, is also shown for comparison. Clearly, the $\Upsilon(2S)$ cascade background cannot produce as narrow a peak as observed in the data. The estimate of the number of $\Upsilon(2S)$ cascade events passing the $\chi_{1D}^2 < 10$ requirement is 1.6–3.0 events (depending on the assumed $\Upsilon(2S)$ product branching ratio). We observe 44 events after this cut in the data. The cross-efficiency for $\pi^0\pi^0$ events

is 0.02% in this sample, which gives a negligible contribution to the signal region. A flat tail in the χ_{1D}^2 distribution for the data, not observed for the signal Monte Carlo, indicates that there is still some background present from other processes like radiative QED events. Since such processes can satisfy the multiple mass constraints built into the χ_{1D}^2 variable only by a random coincidence, the distribution of that background varies slowly in χ_{1D}^2 except for the bias towards lower values introduced by the χ_{1D}^2 minimization with respect to $M_{\Upsilon(1D)}$, J_{2P} and J_{1P} . We use the $\Upsilon(3S) \rightarrow \pi^0\pi^0\Upsilon(1S)$ Monte Carlo (with the π^0 veto cuts removed) as a model of the χ_{1D}^2 distribution for this background component (see Fig. 6). Normalization of this background is fixed from the observed tail of the χ_{1D}^2 distribution. This shape is likely to overestimate the amount of bias in χ_{1D}^2 towards the lower values since, unlike the $\Upsilon(3S) \rightarrow \pi^0\pi^0\Upsilon(1S)$ process, the QED backgrounds do not automatically satisfy the $M_{\Upsilon(3S)} - M_{\Upsilon(1S)}$ mass constraint built into the chi-squared variable. Therefore, we also used a linear background model, with the line parameters fixed by a fit to the tail of the χ_{1D}^2 distribution. Depending on the background shape model, the $\chi_{1D}^2 < 10$ sample has a 9.5 – 13.9% background rate (including the $\Upsilon(2S)$ cascade background). A fit of the $\Upsilon(1D)$ signal, on top of the backgrounds, is shown in Fig. 7. The $\Upsilon(2S)$ background contribution was fixed from the Monte Carlo simulations. Normalization of the other backgrounds was left as a free parameter in the fit. The fit gives a signal amplitude of 40.7 ± 6.8 events. If we try to fit the data with the background contribution alone, the likelihood value of the fit drops dramatically. From the change of the likelihood we estimate that the signal has a significance of 9.7 standard deviations. Significant signals are observed in the $\gamma\gamma\gamma\gamma e^+e^-$ and $\gamma\gamma\gamma\gamma\mu^+\mu^-$ subsamples taken separately (5.2σ and 8.2σ , respectively).

V. MASS ANALYSIS

To turn the observed signal yield into a signal branching ratio, we need to estimate the signal efficiency. Even though the signal shape in the χ_{1D}^2 variable is fairly independent of the masses and spins of the produced $\Upsilon(1D)$ states, the selection efficiency does depend on these parameters via the cuts used to suppress the $\Upsilon(2S)$ cascade background. This is illustrated in Fig. 8, where we plot the selection efficiency as a function of the mass of the $\Upsilon(1D)$ state. Three different curves are presented, for $J_{1D} = 1, 2$ and 3. The $J_{1D} = 2$ state is predicted by Godfrey and Rosner [7] to be produced with the highest rate, $2.6 \cdot 10^{-5}$. The $J_{2P} = 1, J_{1P} = 1$ combination is predicted to be the main production and decay path for this state. The selection efficiency for the $J_{1D} = 2$ state gradually increases with its mass, but is reasonably high in the entire search window. The $J_{1D} = 3$ state, predicted with a $0.8 \cdot 10^{-5}$ rate, can only be produced via the $J_{2P} = 2, J_{1P} = 2$ combination due to angular momentum conservation. This happens to be an unfortunate combination, since for a wide range of masses such a production fakes the $\Upsilon(2S)$ cascade, and the detection efficiency after the $\Upsilon(2S)$ suppression cuts is very low. We become sensitive to this state only if its mass exceeds about 10170 MeV/ c^2 . Finally, the $J_{1D} = 1$ state is predicted by Godfrey and Rosner to have the lowest product branching ratio, $0.4 \cdot 10^{-5}$. This state is again predicted to be produced mostly via the $J_{2P} = 1, J_{1P} = 1$ combination, and therefore our efficiency for this state is similar to the $J_{1D} = 2$ efficiency.

A straightforward way to measure the mass of the produced $\Upsilon(1D)$ state is to calculate the mass of the system recoiling against the two lowest energy photons in the event. The distribution of the difference between the center-of-mass energy and this recoil mass, $E_{CM} - M_{recoil\gamma_1\gamma_2}$, which should peak at $M_{\Upsilon(3S)} - M_{\Upsilon(1D)}$, is shown for the Monte Carlo simulation

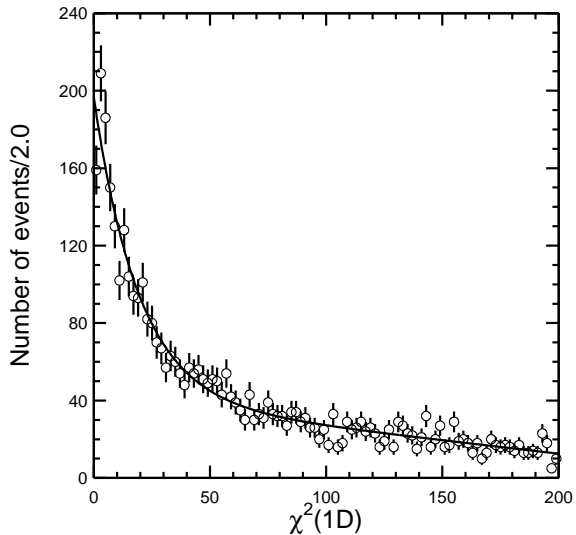


FIG. 6: Fit of a smooth curve to the χ_{1D}^2 distribution observed for the $\Upsilon(3S) \rightarrow \pi^0 \pi^0 \Upsilon(1S)$ Monte Carlo, with the π^0 veto cuts removed.

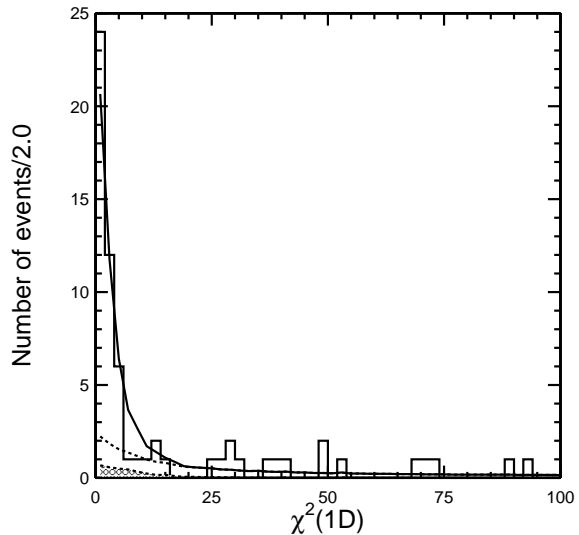


FIG. 7: Fit to the χ_{1D}^2 distribution in the data. The solid-line represents the fit of the signal contribution on top of the backgrounds. The dashed-line represents the total background contribution. The dashed-shaded area shows the $\Upsilon(2S)$ cascade background.

of a $\Upsilon(1D_2)$ state with a mass of $10160 \text{ MeV}/c^2$ in Fig. 9. This distribution can be well described with a Gaussian that has a power-law tail on the low side (a so-called Crystal Ball Line Shape), as illustrated in Fig. 9. The asymmetric tail is caused by transverse and longitudinal shower energy leakage in the calorimeter. The Gaussian part has a resolution of $\sigma = (6.8 \pm 0.3) \text{ MeV}/c^2$.

The mass value that minimizes χ_{1D}^2 is also an estimate of the true $\Upsilon(1D)$ mass. The distribution of this mass for the same Monte Carlo sample as above is shown in Fig. 10. A narrow peak at the correct mass is observed with a resolution of $\sigma = (3.1 \pm 0.1) \text{ MeV}/c^2$. The mass resolution is improved in this method due to the constraints from the well measured masses of the P states built into the χ_{1D}^2 variable. Unfortunately, there are also two satellite peaks, one on each side of the main peak. These false peaks originate from photon energy fluctuations which can make a wrong J_{2P}, J_{1P} combination produce the smallest chi-squared value.

The distributions of $E_{CM} - M_{recoil \gamma_1 \gamma_2}$ and the $\Upsilon(1D)$ mass which minimizes χ_{1D}^2 for each event (called the most-likely mass) are shown for the data in Figs. 11-12 after the $\chi_{1D}^2 < 10$ cut. The background fraction for this sample is in the 9 – 14% range. Two peaks are observed in the distribution of the most likely mass, around 10160 and $10175 \text{ MeV}/c^2$. The recoil mass distribution does not show a double-peak structure, but the mass resolution is worse in this variable, as discussed above.

To analyze the most likely mass distribution, which has a better mass resolution, we fit the data to either a two-peak or a one-peak (positioned either around 10160 or $10175 \text{ MeV}/c^2$)

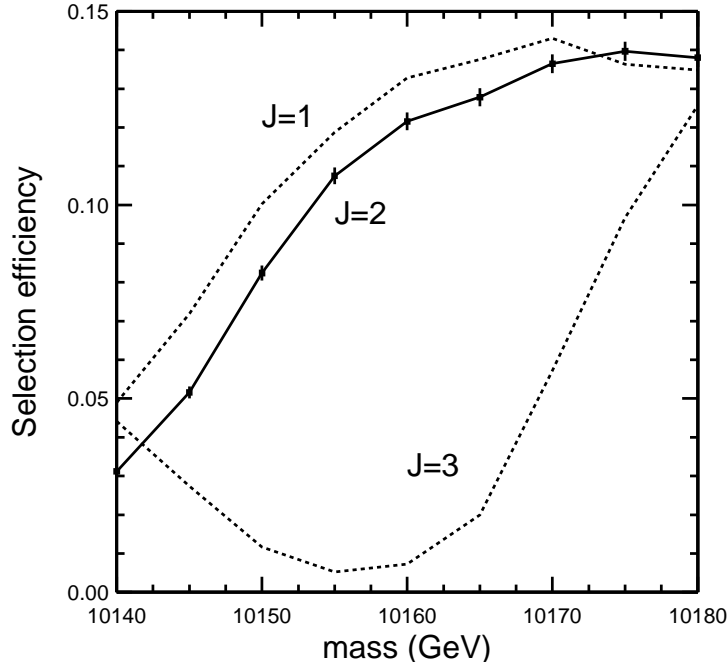


FIG. 8: Selection efficiency (with the $\chi^2_{1D} < 10$ cut included) for $\Upsilon(1D)$ states of different J_{1D} as a function of the mass of the state.

hypothesis. The background is assumed to have a flat distribution. Since the backgrounds are not significant, their parameterization is rather unimportant. Because, in principle, up to three triplet $\Upsilon(1D)$ states can contribute to our sample, we also tried to force a third peak into the fit function. However, the fit either makes the amplitude of this peak zero, with no effect on the amplitudes of the other two peaks, or the third peak collapses into one of the other two peaks. The two-peak fit, displayed in Fig. 13, gives the best confidence level (58%). The amplitude (mass) of the first peak is $27.8^{+6.8}_{-6.0}$ events (10161.2 ± 0.7 MeV/ c^2), and of the second peak $12.0^{+5.3}_{-4.6}$ events (10174.2 ± 1.3 MeV/ c^2). The assumption that there is no peak around 10160 MeV/ c^2 produces a very low confidence level (0.04%) and can be ruled out. From the change of likelihood between these two fits, the significance of the first peak is 6.8 standard deviations. The hypothesis of just one peak around 10160 MeV/ c^2 also produces a good confidence level of 43% (see Fig. 14), with $38.6^{+6.8}_{-6.2}$ events in the peak (10162.0 ± 0.5 MeV/ c^2 mass). Furthermore, while the recoil mass distribution is consistent with the production of two states with the amplitudes and masses as determined by the fit above (confidence level 36%), it prefers to allocate most of the events to the lower mass state, $37.7^{+8.5}_{-7.5}$, with only $2.9^{+5.8}_{-5.2}$ events attributed to the higher mass state, when the amplitudes are let free in the fit. This fit is displayed in Fig. 15 and has a confidence level of 48%. The single-peak interpretation of the recoil mass distribution also has a high confidence level (50%), with $40.5^{+6.9}_{-6.3}$ events at a mass of 10163.4 ± 1.3 MeV/ c^2 (Fig. 16).

In the region of the first peak in the most likely mass distribution, $(77 \pm 9)\%$ of the events have the $J_{2P} = 1$, $J_{1P} = 1$ combination as the most likely. This is consistent with the Monte Carlo simulations for both the $\Upsilon(1D_2)$ (78%) and $\Upsilon(1D_1)$ (73%) states. Furthermore, we

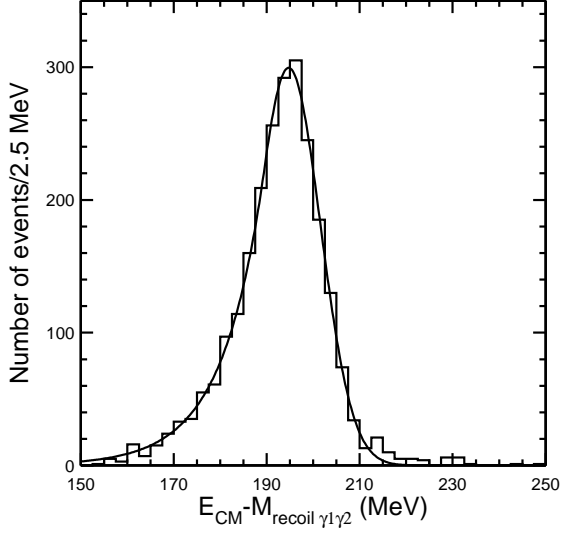


FIG. 9: Distribution of the difference between the center-of-mass energy and the recoil mass against the two lowest energy photons for the $\Upsilon(1D_2)$ Monte Carlo events generated with a mass of $10160 \text{ MeV}/c^2$. The solid-line illustrates the fit of the Crystal Ball Line Shape to the distribution.

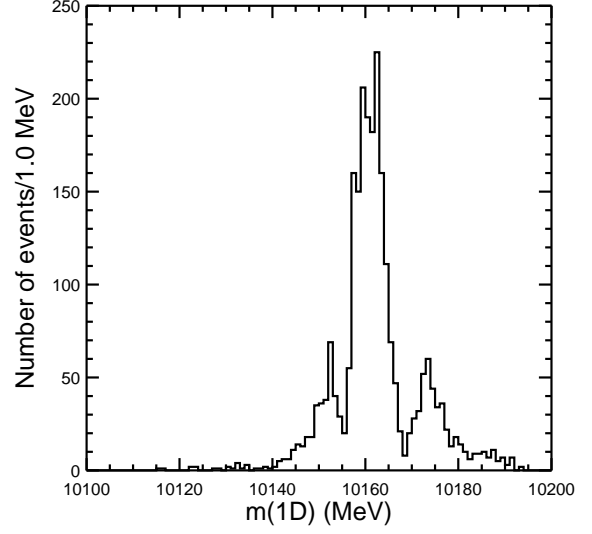


FIG. 10: Distribution of the most likely mass assignment for the $\Upsilon(1D_2)$ Monte Carlo events generated with a mass of $10160 \text{ MeV}/c^2$. In addition to the narrow peak at the correct mass, two satellite peaks at lower and higher mass are produced.

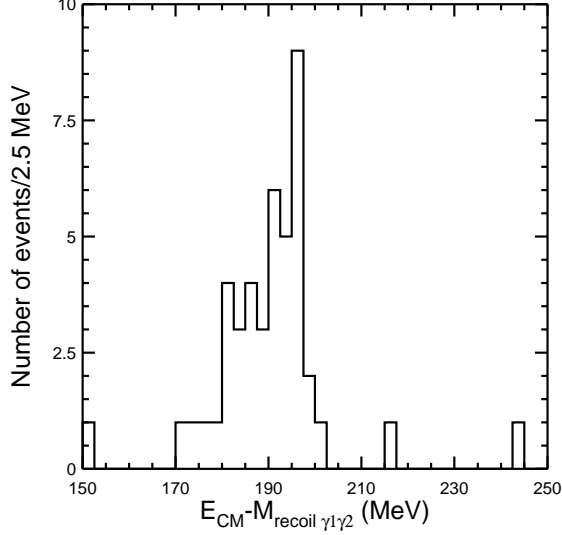


FIG. 11: Distribution of the difference between the center-of-mass energy and the recoil mass against the two lowest energy photons for the data.

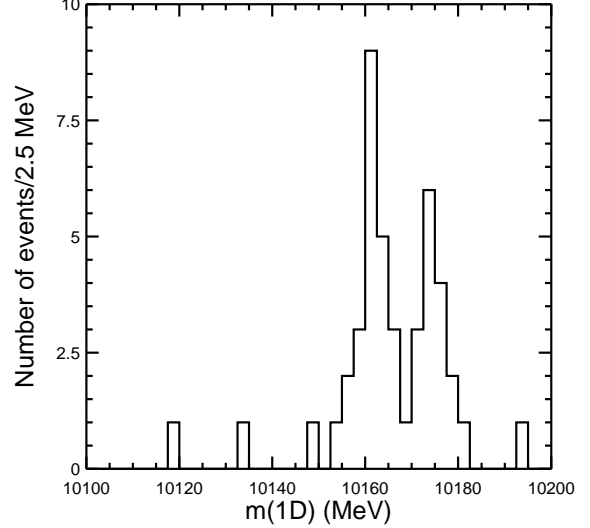


FIG. 12: Distribution of the most likely mass assignment for the $\Upsilon(1D)$ candidate events in the data.

have very low efficiency for the $\Upsilon(1D_3)$ state at this mass (Fig. 8). When we remove the cuts suppressing the $\Upsilon(2S)$ cascades, which are responsible for the efficiency loss for the $\Upsilon(1D_3)$ state, the amplitude of this peak does not increase dramatically. Therefore, this cannot be the $J_{1D} = 3$ state. The $\Upsilon(1D_2)$ state is predicted to be produced with a 6 times larger rate than the $\Upsilon(1D_1)$ state [7]. The Clebsch-Gordan coefficients play a big role in this ratio, thus the model dependence of this prediction is weak. Therefore, we take the $\Upsilon(1D_2)$ state as the most likely interpretation of the first peak. Taking an average over the different fits described above, we measure mass of this state to be $10162.2 \pm 1.6 \text{ MeV}/c^2$. The error is dominated by the dependence on the fit approach ($\pm 1.2 \text{ MeV}/c^2$), with smaller contributions from the statistical error ($\pm 0.7 \text{ MeV}/c^2$), photon energy scale error ($\pm 0.7 \text{ MeV}/c^2$) and the uncertainty on the $\Upsilon(3S)$ mass ($\pm 0.5 \text{ MeV}/c^2$). Predictions of the most successful potential models predict the center-of-gravity of the $\Upsilon(1D)$ triplet to be around this mass [7]. Calculations of the fine splitting of the $\Upsilon(1D)$ states predict the $J_{1D} = 2$ state to be close to the center-of-gravity mass [7]. Our mass measurement is consistent with these predictions.

Only 3 events have $J_{2P} = 2$, $J_{1P} = 2$ as the most likely combination. If the $J_{1D} = 3$ state was produced with the amplitude of 12 events, as suggested by the two-peak fit to the distribution of the most likely mass, we would expect 9.4 such events, including 1.5 events of feed-down from the $\Upsilon(1D_2)$ state at $10162 \text{ MeV}/c^2$. As described previously, the recoil mass distribution shows no evidence for a state at $10174 \text{ MeV}/c^2$ either. Thus, there is no strong evidence for the second state in our data. More data, which will be accumulated by CLEO III at the $\Upsilon(3S)$ in the future, will help to clarify the interpretation of these results.

VI. INCLUSIVE PRODUCTION RATE FOR THE $\Upsilon(1D)$ STATES

To calculate the signal efficiency in the fit to the χ_{1D}^2 distribution (Fig. 7), we weight the $\Upsilon(1D_2)$ efficiency for a state with a mass of $10160 \text{ MeV}/c^2$ and the $\Upsilon(1D_3)$ efficiency for a state with a mass of $10175 \text{ MeV}/c^2$ in a ratio proportional to the observed peak amplitudes in the two-peak fit to the observed most likely mass distribution. We use the difference between this weighted efficiency and the individual efficiencies for each state as an estimate of the systematic error. This gives an efficiency of $(13.2 \pm 1.0)\%$. Converting the number of $\Upsilon(1D)$ events determined by the fit to the χ_{1D}^2 distribution to a product branching ratio, we obtain $(3.3 \pm 0.6 \pm 0.5) \cdot 10^{-5}$. This is an inclusive rate that sums over all possible $\Upsilon(1D)$ states. This rate is in good agreement with the $3.76 \cdot 10^{-5}$ prediction by Godfrey and Rosner [7].

VII. SUMMARY

In summary, we present evidence at the 9.7 standard deviation significance for production of $\Upsilon(1D)$ states in four-photon cascades from the $\Upsilon(3S)$. The inclusively measured product branching ratio, $\mathcal{B}(\Upsilon(3S) \rightarrow \gamma\chi_b(2P)) \cdot \mathcal{B}(\chi_b(2P) \rightarrow \gamma\Upsilon(1D)) \cdot \mathcal{B}(\Upsilon(1D) \rightarrow \gamma\chi_b(1P)) \cdot \mathcal{B}(\chi_b(1P) \rightarrow \gamma\Upsilon(1S)) \cdot \mathcal{B}(\Upsilon(1S) \rightarrow l^+l^-) = (3.3 \pm 0.6 \pm 0.5) \cdot 10^{-5}$, is in good agreement with the theoretical predictions by Godfrey and Rosner [7], where $\mathcal{B}(\Upsilon(1S) \rightarrow l^+l^-)$ above means the average branching ratio over e^+e^- and $\mu^+\mu^-$. From the observed mass distribution we see a 6.8 standard deviation signal for a state with a mass of $10162.2 \pm 1.6 \text{ MeV}/c^2$. This is likely to be the $J_{1D} = 2$ state, though we cannot rule out the $J_{1D} = 1$ hypothesis. However,

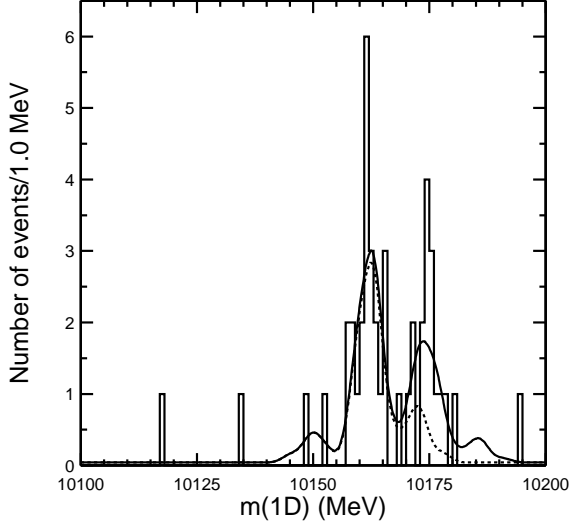


FIG. 13: The fit (solid-line) of a two-peak structure to the observed distribution of the most likely mass. The dashed-line indicates the fitted contribution of the first peak plus the background. The signal shape for each peak has a central peak, and a smaller satellite peak on each side of the central peak.

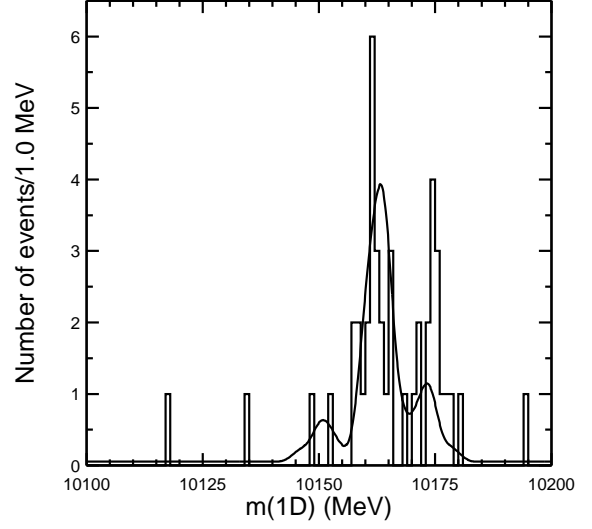


FIG. 14: The fit (solid-line) of one-peak structure to the observed distribution of the most likely mass.

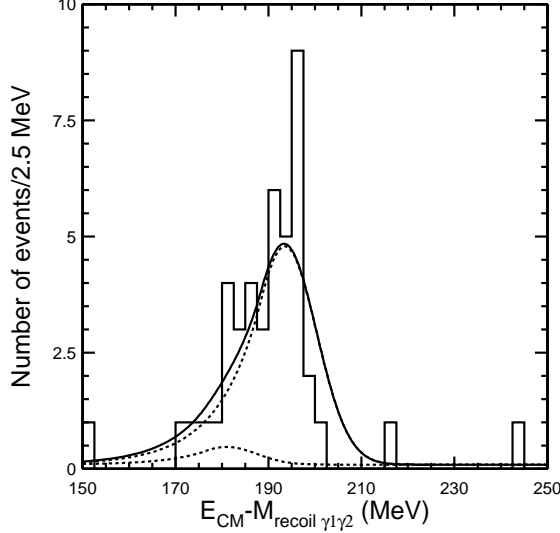


FIG. 15: The fit (solid-line) of a two-peak structure to the distribution of $E_{CM} - M_{recoil \gamma_1 \gamma_2}$. The peak positions were fixed to the masses obtained by the fit to the most likely mass (the higher mass state appears at a lower value of $E_{CM} - M_{recoil \gamma_1 \gamma_2}$). The amplitudes of the peaks were allowed to float. The dashed-lines indicate the fitted contributions of each peak separately.

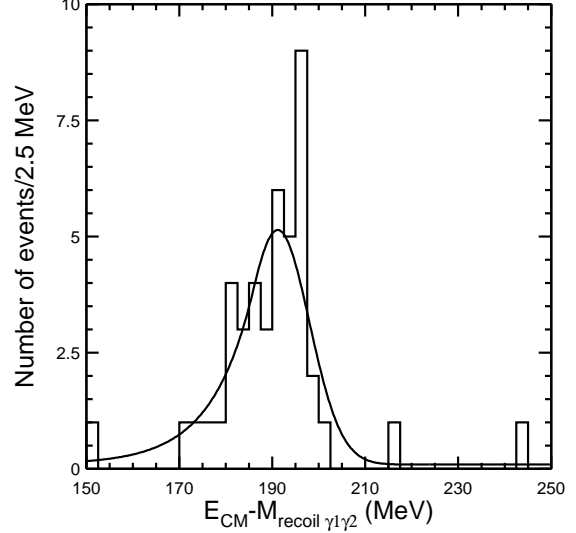


FIG. 16: The fit (solid-line) of a one-peak structure to the observed distribution of the difference between the center-of-mass energy and the recoil mass against the two lowest energy photons. The amplitude and peak positions were free parameters in the fit.

the $J_{1D} = 1$ hypothesis is strongly disfavored by theoretical expectations. Evidence for a second heavier state in our data is so far inconclusive. This is the first discovery of an $L = 2$ quarkonium state below the open flavor threshold.

We gratefully acknowledge the effort of the CESR staff in providing us with excellent luminosity and running conditions. We thank J. L. Rosner for the useful discussions concerning the $\Upsilon(1D)$ states. M. Selen thanks the PFF program of the NSF and the Research Corporation, and A.H. Mahmood thanks the Texas Advanced Research Program. This work was supported by the National Science Foundation, and the U.S. Department of Energy.

-
- [1] See e.g. C. T. Davies *et al.* (UKQCD Collaboration), Phys. Rev. **D58**, 054505 (1998) and references therein.
 - [2] For reviews see e.g. D. Besson and T. Skwarnicki, Ann. Rev. Nucl. Part. Sci. **43**, 333 (1993); E. Eichten and C. Quigg, Phys. Rev. **D49**, 5845 (1994).
 - [3] S. W. Herb *et al.*, Phys. Rev. Lett. **39** (1977) 252; W. R. Innes *et al.*, Phys. Rev. Lett. **39**, 1240 (1977) [Erratum-*ibid.* **39**, 1640 (1977)].
 - [4] K. Han *et al.* (CUSB), Phys. Rev. Lett. **49**, 1612 (1982); G. Eigen *et al.*, Phys. Rev. Lett. **49**, 1616 (1982).
 - [5] C. Klopfenstein *et al.*, Phys. Rev. Lett. **51**, 160 (1983). and Ref. [6].
 - [6] F. Pauss *et al.* (CUSB), Phys. Lett. B **130**, 439 (1983).
 - [7] S. Godfrey and J. L. Rosner, Phys. Rev. **D64**, 097501 (2001); see also W. Kwong and J. L. Rosner, Phys. Rev. **D38**, 279 (1988) and other references therein.
 - [8] G. Crawford *et al.* (CLEO II), Phys. Lett. **294B** (1992) 139.
 - [9] U. Heintz *et al.* (CUSB), Phys. Rev. **D46** 1928 (1992). We corrected the $\mathcal{B}(\Upsilon(3S) \rightarrow \pi^0\pi^0\Upsilon(1S))$ published in this paper to the value of $\mathcal{B}(\Upsilon(1S) \rightarrow l^+l^-)$ used in our calculations.
 - [10] Y. Kubota *et al.*, Nucl. Instrum. Meth. **A320**, 66 (1992).
 - [11] D. Peterson *et al.*, Nucl. Instrum. Meth. **A478**, 142 (2002).
 - [12] “Study of Two-Photon Transitions in CLEO III $\Upsilon(3S)$ Data”, G. Bonvicini *et al.* (CLEO), paper submitted to this conference, ICHEP02 ABS949, CLEO CONF 02-07.
 - [13] K. Hagiwara *et al.* (Particle Data Group) Phys. Rev. **D66**, 010001 (2002).
 - [14] F. Butler *et al.* (CLEO II), Phys. Rev. **D49**, 40 (1994). We corrected the $\mathcal{B}(\Upsilon(3S) \rightarrow \pi^0\pi^0\Upsilon(1S))$ published in this paper to the value of $\mathcal{B}(\Upsilon(1S) \rightarrow l^+l^-)$ used in our calculations.
 - [15] Ref. [6] and W. Walk *et al.* (Crystal Ball), Phys. Rev. **D34**, 2611 (1986).